Investigation of adsorption properties of modified DD kaolins to microporous material type 13X zeolite in treatment of textile industry effluent: experiments and theoretical approach

Ibtissem Slatni, Asma Dhiffalah, Fatima Zohra Elberrichi, Nor El Houda Fardjaoui, Abdelkrim Guendouzi, Joelle Duplay, Brahim Gasmi, Ammar Maoui

Investigation of adsorption properties of modified DD kaolins to microporous material type 13X zeolite in treatment of textile industry effluent: experiments and theoretical approach

Ibtissem Slatni [1] · Asma Dhiffalah[2] · Fatima Zohra Elberrichi[1] · Nor El Houda Fardjaoui[1] · Abdelkrim Guendouzi[3,4] · Joelle Duplay [5] · Brahim Gasmi[6] · Ammar Maoui[1]

[1] Laboratoire Génie Civil et d′hydraulique, Université 8 Mai 1945, BP401, Guelma, Algeria
[2] Département des Sciences de la Matière, Université 8 Mai 1945, BP401, Guelma, Algeria
[3] Laboratory of Chemistry, Synthesis, Properties and Applications, University Dr Moulay Tahar, Saida, Algeria
[4] Laboratory of Applied Thermodynamics and Modeling Molecular, University Abou Bekr Belkaid, Tlemcen, Algeria
[5] Institut Terre et Environnement Strasbourg (ITES) – UMR 7063 - Ecole et Observatoire des Sciences de la Terre, (EOST), 5, rue Descartes, 67084 Strasbourg Cedex, France
[6] Laboratoire de Physique des couches minces et Application, Université Mohamed Khider, Biskra, Algeria

Abstract

The textile industry has experienced a great development accompanied by a large production of polluted water released into the environment, which requires a treatment that varies according to the nature of the pollutants. The work carried out aims at testing 13X type zeolites synthesized from Djebel Debagh DD1, DD2, and DD3 kaolins in order to remove dyes and other pollutants from the effluent of the COTITEX textile industry (Batna, Algeria). Several experimental parameters were studied (pH, temperature, initial concentration, mass of adsorbent) and physicochemical characterizations were done on the synthesized adsorbents and the effluent to be treated.

The zeolites 13X synthesized from DD1, DD2, and DD3 kaolins were characterized using X-ray diffraction (XRD), Fourier transforms infrared (FTIR), and scanning electron microscopy (SEM). The adsorption experiments were done using the anionic dye present in the effluent and using real textile effluent. The results show that the dye adsorption is efficient and feasible at ambient temperature on the 13X type zeolite synthesized from DD1 kaolin compared to 13X zeolites synthesizedfromDD2 and DD3, with a good discoloration efficiency. Experiments with real textile wastewater showed a significant improvement in the physicochemical characteristics (COD, DBO_5, TSS, PO_4^{3-}, and NO_2^-) compared to the untreated effluent.

Key words: 13X type zeolite, Djebel Debagh Kaolin DD, Anionic dye, Adsorption, Real textile effluent.

1. Introduction

Industrial activities are a very important source of pollution and contribute in some way to the deterioration of the environment. The discharges of the textile industry constitute enormous nuisances for human health, in particular the various dyes which are used in excess. As a result, the wastewater is strongly colored and concentrated in these organic molecules whose effect is harmful to human health and the environment.

Various conventional methods have been used to remove pollutants from water; the most popular methods are physical-chemical or chemical-biological methods such as coagulation, flocculation, precipitation and membrane filtration, and adsorption which is the most effective process for dye removal. Activated carbon is an effective adsorbent but its cost is high. Contrary, clays are at low cost and have the advantage of being able to be modified or even to be transformed into micro-mesoporous material of the zeolite-type to improve their adsorption capacity. Indeed, zeolites have been suggested and studied to overcome many drawbacks through their greater stability over a wide range of temperatures and pressures, lower energy requirements, and lower costs (Chowdamet al. 2016; Sandeep et al. 2015; Schwankeet al. 2019).

Many works pointed out the adequacy of fly ash as feedstock in the synthesis of zeolites (Shigemoto et al. 1993; Singer et al. 1995). However, to lower the costs, natural kaolin has begun to be used in the synthesis of these microporous and mesoporous materials. The synthesis of kaolinite based zeolite is well-known and described by Barrer et al**.** (1974) and more recent studies and reviews (Akolekar et al. 1997; Candamano et al. 2019; Fardjaoui et al. 2017; Hartati et al. 2020; Schwanke et al. 2019; Villaquirán-Caicedo et al. 2016).

Further raw materials such as high silica bauxites, halloysites, and montmorillonites are also used for the synthesis of zeolites (Aiello et al. 1984). Nevertheless, to the best of our knowledge, no previous study has been done on the use of the natural Algerian Djebel Debagh (DD) kaolins in the East of Algeria as starting material to directly synthesize zeolite. Algeria is a country with many deposits of kaolin that can be used as a material for environmental pollution control and industrial effluent treatment. The kaolin of Djebel Debagh, in particular, is found in abundant quantity.

On the other hand, the existing literature on the adsorption of anionic dyes and the treatment of real industrial effluent using zeolite and mesoporous materials is scarce and limited (Fardjaoui et al. 2017; Slatni et al. 2020).

This study will focus on the synthesis of 13X zeolite from Djebel Debagh natural kaolins (DD1, DD2, DD3), and on the capacities of these clays and synthesized zeolites to adsorb commercial anionic dye (Bezanyl Yellow) and treat a raw effluent supplied by the Batna textiles company "EATIT" (Fardjaoui et al. 2017).

The DD natural kaolins and the 13X zeolite synthesized from theses kaolins were studied for dye and textile effluent adsorption efficiency, and their characteristics such as crystal morphology, framework structure, and pore structure were examined by XRD, SEM, BET and FTIR.

Moreover, a theoretical and computational study of the interaction between dye and zeolite was performed. It is based on the enormous power of DFT (density functional theory) calculations (Casaburi et al. 2021; Curcio et al. 2018), as one of the most important modeling techniques to understand the intercalation process in adsorption phenomena (Ramdani, et al. 2020; Slatni et al. 2020), which has been greatly improved by their applications to organic materials and inorganic adsorption design (Petrosino et al. 2019, 2020)

2. Experimental work

2.1 Materials

Djebel Debagh's kaolin or kaolin DD is natural kaolin exploited for almost a century for fine ceramics, pottery, and refractory material. It is extracted from a hydrothermal deposit located at Djebel Debagh in the wilaya of Guelma (Algeria). The DD kaolins are classified into 3 categories or grades according to their qualities and composition: DD1, DD2, and DD3.

Bezanyl Yellow is an acid dye in the form of salt, belonging to the category of water-soluble dyes. It was supplied by SOITEX Algerian Textile Company of Tlemcen (Algeria). This dye is used for textiles dyeing, especially polyamide fibers. The characteristics of Bezanyl Yellow are shown in **Table 1**.

The textile industry effluent used in the present study was supplied by EATIT (a company specializing in the printing of military uniforms) and contains a mixture of vat dyes and auxiliaries.

Table 1: Properties and characteristics of Bezanyl Yellow

Type	Anionicdye
Nature	Acid
Name according to IUPAC	2- [4- [2- (1-anilino-1,3-dioxobutan- ylidene) hydrazinyl] phenyl] -6-methyl-1,3-benzothiazole-7-sulfonate
Chemical formula	$C_{24}H_{19}N_4NaO_5S_2$
Molecular weight	530.05 g / mol

λ_{max}	435 nm
Chemical structure	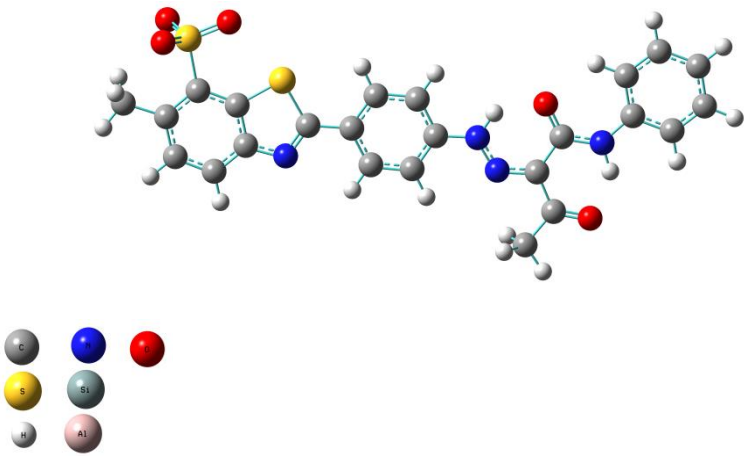

2.2.Synthesis of Zeolite type 13X

2.2.1 Preliminary treatment of natural kaolin DD

The preliminary treatment of DD1, DD2, and DD3 natural kaolins consists in making rid of all the minor crystalline phases (quartz, calcite, feldspar) by screening. The kaolins underwent further preliminary operations: crushing, drying in the oven at T = 80 °C for 24 hours, and sieving.

2.2.2 Synthesis of 13X zeolite from kaolin DD

The synthesis of the 13X zeolite from DD kaolin consists of alkaline fusion followed by hydrothermal treatment. Alkaline fusion: a 2:1 ratio of sodium hydroxide was mixed with the DD kaolin in a crucible at 200 °C for 4 hours. Then the mixture was cooled until reaching room temperature and added to water and homogenized through vigorous stirring for 2 h at 50 °C. The crystallization is obtained at 90 °C while stirring for 8 hours (300 rpm). Finally, the solid was filtered and washed several times with distilled water until pH = 8 and dried at 105 °C.

2.3 Methods

The chemical composition of materials was determined using a PANalytical Magic PROX–ray fluorescence spectrometer equipped with a chromium tube and five analyzing crystals, namely LIF 200, LIF 220,

GE, PE, and PX 65. The detectors are a combination of gas-flow proportional counter and a scintillation detector. The gas-flow proportional counter uses P10 gas, which is a mixture of argon and methane at a 9/1 ratio.

X-ray diffraction (XRD) of the random-powdered clays and zeolites was carried out by using the XRD instrument X-Pert Propanalytical diffractometer using Ni filtered Cu-Kα radiation source (λ= 1.5, 406 Å, 30 kV, 30 mA, and automatic mono-chromator). The diffractograms were recorded in the range 2θ= 10-70 °, with a scanning rate of 1°/min.

The surface morphologies of DD kaolins and zeolites were examined by Scanning Electron Microscopy (SEM; JSM-6390 LU, JEOL, Biskra, Algeria operating at 5–30 kV). To examine these materials, the samples were coated with a conducting layer of gold and carbon by sputter coating.

Fourier Transform Infrared (FTIR) spectra of materials were carried out on powdered samples mixed in KBr pellets in the range 4000- 400 cm^{-1} using a spectrophotometer BRUKER IFS 66 v/S.

Effluent's conductivity was determined by Thermo Scientific Orion Star A215 pH/ Conductivity Benchtop Meter. The pH measurements were done using HANNA instrument according to the standard ISO 10523.2008.

Chemical oxygen demand (COD mg O_2/L) was measured as per standard procedures (APHA 1998) using Hach Lange cuvette tests (LCK314 and LCK614, with a range of 0–150 mg/L O_2 and 50–300 mg/L O_2, respectively), and the WTW spectral photolab spectrophotometer. The cuvettes containing the pre-dosed reagents were incubated at 148 °C for 2 h before measurement. The concentrations of $NH_4^+$and NO_2^-, PO_4^{3-}, and SO_4^{2-}were measured at wavelengths, λ=500 nm, λ= 880 nm, and λ= 450nm, respectively, using the LCK cuvette tests and WTW spectral photolab spectrophotometer.

Total suspended solids (TSS) in the effluent were measured by filtering a known volume of effluent sample, drying the filter with the captured solids, and then weighing the filter to determine the weight of the captured suspended solids. The entire process takes about 2 hours and does not allow instantaneous and continuous measurement (NF EN 872.2005).

The oxygen content of the water BOD_5 is determined immediately after sampling, then again after an incubation time of 5 days at 20 °C. The difference between the two measurements corresponds to oxygen consumption, considered under these conditions as biochemical oxygen demand (AFNOR NF EN 1899-2 standard. 1998).

2.4 Adsorption experiments

2.4.1 Textile dye adsorption

The batch experiments of adsorption kinetic studies were performed by mixing 200 mL of Bezanyl Yellow at the initial concentration of Co = 25 mg /L with 0.1 g of adsorbent. The mixtures were homogenized at a constant stirring speed of 400 rpm. Dye adsorption kinetics was investigated at 20 ˚C and natural pH for 120 min. Samples were collected at different time intervals: 2 mL of liquid were taken from the suspension and were then centrifuged for 15 min at 5000 rpm, and the left out concentration in the supernatant solution was analyzed through UV visible at the wavelength of maximum absorbance of the dye.

The residual concentration of each sample allows determining the quantity of fixed dye per gram of adsorbent according to equation (1):

$$\boldsymbol{Q_t = (C_0 - C_t) * V/m} \text{.....(1)}$$

It is also possible to evaluate the quantity adsorbed by the adsorption yield given by equation (2):

$$\boldsymbol{P}(\%) = \boldsymbol{(C_0 - C_t) * 100/C_0} \text{ ……..(2)}$$

where, Q_t is the amount of adsorbed ions per unit adsorbent at the time t (mg/g); m is the mass of adsorbent used (g); C_0 represents the initial concentration of dye in solution (mg/L); C_t is the concentration of dye in solution at the time t (mg/L), and V is the volume of solution used (L).

Kinetic models

Various kinetics models have been used in the literature to assess the adsorption process (Li et al. 2009; Doğan et al. 2006; Ho and McKay, 2000). The most common kinetic models used to monitor the kinetics of adsorption processes are Lagergren's pseudo-first-order model and Ho's pseudo-second-order model, while interfacial and particle diffusion models are most commonly used to determine the mechanism of adsorption .

They have been widely used in dye adsorption studies on synthetic or natural zeolites which are mostly modified or as a composite material. Studies on unmodified natural or synthetic zeolites as adsorbents of anionic dyes are rarer (de Carvalho et al., 2011; Xu et al., 2014; Colachite Rodrigues Bertolini et al., 2015; Fardjaoui et al., 2017; Liang et al., 2021; Radoor et al., 2021; Tabti et al. 2021).

In all these few studies, it is the pseudo-second order kinetic model that best describes the experimental data, except in one study (Xu et al., 2014) where a multi-step process occurs described by the pseudo-first-order model during the first step followed by a second step controlled by the intra-particle diffusion mechanism.

Lagergren pseudo–first-order model

The model based on the assumption that the rate of change of solute uptake with time is directly proportional to (Qe- Qt) (Lagergren, 1898) which is generally more suitable for lower concentrations of solute, and is expressed by the following relation:

$$\frac{dQ_e}{dt} = K_1(Q_e - Q_t) \dots\dots\dots\dots\dots\dots\dots\dots (3)$$

Where K_1 is the equilibrium rate constant in the pseudo–first-order model (L/min). Définir Q_e Q_t

After integration, the following equation is obtained:

$$\ln(Q_e - Q_t) = lnQ_t - K_1 t \dots\dots\dots\dots (4)$$

Pseudo-second-order

The rate of pseudo-second-order reaction is dependent on the amount of solute adsorbed on the surface of adsorbent and the amount adsorbed at equilibrium (Ho, 1995) The pseudo-second order model can be represented in the following form:

$$\frac{dQ_e}{dt} = K_2(Q_0 - Q_t)^2 \dots\dots\dots\dots (5)$$

Where K_2 is the rate constant of pseudo-second-order model (g/mol min). définir Q_0 , Q_t et Q_e

After integrating Eq. (5) the following equation can be obtained:

$$\frac{t}{Q_t} = \frac{1}{K_2 Q_e^2} + \frac{t}{Q_e} \dots\dots\dots\dots\dots\dots\dots (6)$$

Intra-particle diffusion

The nature of the rate-limiting step in a batch system can also be assessed from the properties of the solute and adsorbent (Doğan et al. 2006). The process of intra-particle diffusion is most likely to be the limiting step that controls adsorption (Kumar and Kacha, 2011).The most widely applied intra-particle diffusion equation for adsorption systems is given by Weber and Morris (1963)

$$Q_t = K_i t^{0.5} + 0.5 \dots\dots\dots\dots\dots (7)$$

Where K_i is intra-particle diffusion rate constant (g/mg min)

Isotherm models

In the aforementioned studies, several isotherm models were tested to describe the experimental data and approach the adsorption mechanism. The Langmuir model describing a monolayer coverage of the dye (de Carvalho et al. 2011; Tabti et al. 2021) and the Freundlich multilayer model (Colachite Rodrigues Bertolini et al. 2015; Fardjaoui et al. 2017; Radoor et al. 2021) are the best to fit the experimental data.

The Langmuir adsorption isotherm (Langmuir 1916) assumes that sorption takes place at specific homogeneous sites within the adsorbent. The linear form of Langmuir isotherm is given by the relation (3):

$$\frac{C_e}{q_e} = \frac{1}{q_m b} + \frac{C_e}{q_m} \qquad \text{eq (3)}$$

where C_e is the equilibrium concentration (mg L^{-1}), q_e the amount adsorbed at equilibrium (mg g^{-1}), q_m the adsorption capacity (mg g^{-1}) and b is the energy of adsorption (Langmuir constant (L mg^{-1}).

The Freundlich adsorption isotherm is based on the adsorption with non-uniform distribution of adsorption heat onto heterogeneous surfaces (Freundlich 1906; Adamson and Gast 1997) as well as multilayer sorption as given by equation (4) below:

$$\log(qe) = \log kF + \frac{1}{n}\log(Ce) \qquad \text{eq (4)}$$

where kF and n are Freundlich constants and were calculated from the slope and intercept of the Freundlich plots ($\log(q_e)$ versus $\log(C_e)$). kF is indicative of the adsorption capacity, and n is the index of adsorption intensity or surface heterogeneity.

Thermodynamic parameters of adsorption

The thermodynamic study reflects the feasibility and spontaneous nature of the adsorption process. The parameters such as free energy (ΔG°), enthalpy variation (ΔH°) and entropy variation (ΔS°) may be estimated from equilibrium constants at different temperatures. The free energy variation of the adsorption reaction is given by:

$$\Delta G° = -RT\ln K_C \quad \ldots\ldots\ldots\ldots\ldots\ldots\ldots (8)$$

Where ΔG° is the variation of free energy (kJ/mol), R is the universal gas constant (8.314 J/mol. K), T is the absolute temperature (K), and Kc is the equilibrium constant.

The values of ΔH° and ΔS° can be calculated from the Van't Hoff equation as follows:

$$lnK_c = -\frac{\Delta H}{RT} + \frac{\Delta S}{R} \dots\dots\dots\dots\dots\dots\dots (9)$$

In most of the aforementioned studies the ΔG° negative values indicate a spontaneous, feasible process, while their value ranges from -20 to 0 kJ mol/1 (Jaycock and Parfitt, 1981) indicate a physisorption process rather than chemisorption.

Treatment of textile effluent

The experiments were conducted using 200 mL of wastewater collected from the textile industry and previously treated by flocculation and coagulation. A magnetic stirrer was used for mixing the effluent at 400 rpm at 20 °C with the adsorbent at natural pH (7 ± 0.5) for 2h and 20 min. The adsorbents used were the three types of DD kaolins (DD1, DD2, DD3) and the 13X zeolites (Z1, Z2, Z3) synthesized from DD1, DD2, DD3 kaolins respectively.

3. Results and discussion

3.1 Characterization of adsorbents

3.1.1 Chemical analysis

The chemical compositions of the studied adsorbents were obtained by ICP-AES analyses. They are given in **Table 2**.

Table 2: Chemical composition of DD1, DD2 and DD3 kaolins

Sample	SiO2	Al_2O_3	TiO2	Fe_2O_3	CaO	MgO	K_2O	LOI[a]
Kaolin DD1	45.31	38.85	0.00	0.01	0.15	0.2	0.02	15.36
Kaolin DD2	43.40	38.89	0.02	0.11	0.21	0.31	0.04	15.89
Kaolin DD3	42.96	37.7	0.03	0.32	0.74	0.23	0.94	16.50

[a]Loss on ignition at 1000°C

From **Table 2**, it can be observed that the raw DD1, DD2, and DD3 kaolins are rich in SiO_2 and Al_2O_3, whereas the loss on ignition (LOI) varies between 15% and 16% for all kaolins due to their dehydroxylation and removal

of the organic and carbonate compounds. However, kaolin DD1 is the richest in silica (45%) and alumina (39%) with the lowest loss on ignition (15%).

3.1.2 X-ray diffraction analysis

Fig 1 illustrates the XRD patterns of the natural kaolins DD1, DD2, and DD3. The diffraction peaks situated at 7.30 Å are attributed to kaolinite; those at 7.40 Å and 7.14 Å are attributed to halloysite, respectively.

It can be seen from **Fig 1** that the major crystalline phases are kaolinite (JCPDS No: 29-1488) in DD1 and DD2, and halloysite (JCPDS No: 29-1487) in DD3.

Fig 1: XRD patterns of DD kaolins

Table 3 shows the clay fraction composition. Besides clay minerals, minor mineral phases such as alunite and natro alunite were identified in DD1 and quartz in DD3.

Table 3: Mineralogical composition of kaolin DD1, DD2, DD3

Sample	Mineralogical composition
Kaolin DD1	✓ Kaolinite ✓ Alunite ✓ Natroalunite
Kaolin DD2	✓ Halloysite ✓ Kaolinite
Kaolin DD3	✓ Halloysite ✓ Kaolinite ✓ Illite ✓ Quartz

From the results of the chemical composition of the kaolins and their mineralogical composition, we have selected DD1 kaolin as our material study for the synthesis of the 13X zeolite because of its kaolinite dominant composition which is mainly used in the literature for 13X zeolite synthesis (Alshahidy et al. 2021; Ma et al. 2014). The XRD patterns of 13X type zeolites Z1, Z2, and Z3 are shown in Fig. 2. The standard 13X zeolite is shown in the inset of Fig. 2(a).

All peak positions of Z1, Z2, and Z3 zeolites matched to those reported for the 13X standard zeolite (Treacy and Higgins; 2007). The diffraction peaks at 2θ = 10.22, 15.5, 20.6, 23, 26.5 of all Z zeolites show respectively the characteristic diffraction peaks (220, 331, 440, 533, 642) which correspond to the typical pattern of crystalline 13X zeolite (Yunan et al. 2014). As some differences in diffraction patterns were identified between Z and 13X standard zeolite, one can assume that the structural framework of 13 X zeolite was obtained with other phases after synthesis from DD kaolin. It can be seen in Fig.2 that the major and predominant crystalline phases are: Faujasite (Baur 1964), Sodalite (Hassan et al. 2004) et Chabazite (Calligaris et al. 1982)

Fig 2: XRD pattern of Z1, Z2, Z3 zeolites and standard 13X zeolite

3.1.3 Fourier transforms infrared analysis

Fig 3 shows the infrared spectra of the Z1, the 13X zeolite synthesized from DD1, and 13X zeolite from the literature (Chen et al. 2012). The detected absorption band around 3459 cm^{-1} in Z1 zeolite corresponds to the structural OH stretching of water molecules that are adsorbed in the zeolite channel (Qiang et al. 2018; Suquet et al. 1989). The band at 1640 cm^{-1} is attributed to H-O-H bending mode due to incomplete dehydration of the zeolite. Moreover, the bands observed at 984 cm^{-1} corresponds to asymmetric stretches (Si-O) or (Al-O). The internal and external linkage symmetric stretches were represented by the 676 cm^{-1} and 755 cm^{-1} bands, respectively. The band observed at 564 cm^{-1} is attributed to double six-member rings (D6R) and the peak at 463 cm^{-1} corresponds to the T-O bend (Chen et al. 2012; Zhan et al. 2002). The same bands were identified for Z1 zeolite and the data obtained from FTIR spectra are in accordance with those reported for 13X zeolite (Chen et al. 2012)**.**

Fig 3: FTIR spectra of Z1 zeolite and 13 X zeolite from the literature (Chen et al. 2012)

3.1.4 SEM analysis

The surface morphologies of the raw kaolin DD1 and Z1 zeolite synthesized from DD1 were examined by scanning electron microscopy **(Fig 4)**.

Fig 4 (a) and (b) show aggregated platelets of a rather uniform size. These structures exhibit large pores offering large adsorption surfaces.

Fig 4 (c) and (d) show clearly the well crystallized Z1 zeolite particles of a uniform 1-2 µm size. These small sized particles offer a large adsorption surface due to their high surface/volume ratio. Moreover, these crystals are

aggregated, forming larger structures of about 10 µm exhibiting a larger pore network compared to DD1, and consequently more important adsorption surfaces.

Fig4: Scanning electron micrographs of DD1 kaolin (a, b) and Z1 zeolite (c, d) at different magnifications

3.2 Adsorption studies of Bezanyl Yellow on DD kaolins and Z zeolites

The adsorption kinetics of Bezanyl Yellow on DD kaolins and on the synthesized Z zeolites were carried out at T = 20 °C. Various parameters were studied, in particular: the contact time, the nature of the adsorbent, the mass of the clay, and the initial concentration of the dye solution.

3.2.1 Influence of contact time on adsorption capacity

Fig 5 shows the Bezanyl Yellow removal evolution with contact time. The curves for the three DD kaolins are similar and their shape indicates a monolayer formation of the dye on the external clay surface (Zen et al. 2018). The removal percentage increased with contact time and reached a maximum value of 100 min where more than 56.8% (28.4 mg/g) of dye could be removed from aqueous solution for DD1 kaolin, 50.4% (25.2mg/g) for DD2, and 44.4% (22.2mg/g) for DD3. After 100 min, the Bezanyl Yellow removal percentage exhibited nearly a plateau curve with slight changes in the uptake capacity reflecting the equilibrium stage, which can be explained by the saturation of the free adsorbent sites of DD kaolins. Therefore, the optimum contact time was considered to be 100 min.The adsorption onto DD1 kaolin was the fastest in the first 10 min, followed by a strong adsorption (56.8%) until reaching equilibrium.

For the removal of dye on Z zeolite (Z1, Z2, Z3) (**Fig 6)**, the adsorption increased for all the Z zeolites compared to DD kaolins. For Z1, it is to notice that more than 90% (45 mg/g) of Bezanyl Yellow could be removed from the aqueous solution within 120 min. The data showed the higher uptake capacity of Z1 for Bezanyl Yellow dye compared to Z2 (76%, 38mg/g) and Z3 (66%, 33mg/g).

It was reported in a previous study, that more than 240 min are needed to achieve equilibrium with DD3 kaolin for 10% removal of Bezanyl Yellow (1.6 mg/g), and 180 min with Zeolite A synthesized from DD3 kaolin for 19% removal of a same dye of (1.8mg/g) (Fardjaoui et al. 2017).

Fig5: Effect of the contact time in the removal of Bezanyl Yellow on DD kaolins (m = 0.1g, pH= 6, C_0= 25 mg/L, T= 20 °C).

Fig 6: Effect of the contact time in the removal of Bezanyl Yellow on Z zeolites (m = 0.1g, pH= 6, C_0= 25 mg/L, T= 20 °C).

3.2.2 Influence of adsorbent nature

Fig 7 shows the effect of the types of kaolin and zeolite on the anionic dye adsorption using 0.1 g adsorbent. The adsorption rates of Bezanyl Yellow on DD1 kaolin and Z1 zeolite are high (60%, 28 mg/g and 90%, 45mg/g respectively) (**Fig 7).** This can be explained by the higher available binding sites of kaolin DD1 which could interact with the number of sorbate ions according to its chemical and mineralogical composition (**Table3)**. Consequently, the Z1 zeolite synthesized from this kaolin would also give the highest removal percentage of anionic dye.

Fig 7: Effect of adsorbent nature on the removal of Bezanyl Yellow dye (m= 0.1g, pH= 6, C_o= 25 mg / L, T= 20 °C)

3.2.3 Effect of the adsorbent mass

The influence of adsorbent dose on the removal of Bezanyl Yellow dye was studied in the range of (0.1-5 g and the results are presented in **Fig 8**, where an increase in the adsorbent mass increases the amount of adsorbed anionic dye. The increase in the adsorption capacity of Z1 zeolite from 90% to 100% and of kaolin DD1 from 78% to 100% is due to the availability of more active sites on the Z1 zeolite than kaolin DD1. It was reported in a previous study that 0.1g of synthesized zeolite A led to the highest Bezanyl Yellow adsorption capacity (2.76 mg/g) (Fardjaoui et al. 2017).

Fig8: Effect of the mass of kaolin DD1 and Z1 zeolite on the adsorption of Bezanyl Yellow, (C_o= 25 mg/ L, pH= 6, T= 20 °C, contact time= 120 min)

3.2.4 Influence of the initial dye concentration

The effect of the initial concentration on the performance of DD1 kaolin and Z1 zeolite is shown in **Fig 9**. The overall trend is an increase in dye removal when increasing the dye concentration. The best results were obtained using 50 mg/L initial dye concentration, where the total Bezanyl Yellow removal percentage reached 80% by DD1 and 98% by Z1 zeolite. At high dye concentration, the number of adsorbed ions that could interact with adsorbent

binding sites increased, hence the anionic dye uptake was enhanced. In a conclusion, the highest removal could be obtained and achieved at a high concentration of anionic dye.

Fig 9: Effect of initial dye concentration of Bezanyl Yellow (m= 0.1 g,pH= 6, T= 20 °C, contact time = 120 min)

3.2.5 Influence of pH

The pH is an important factor in any dye adsorption study since it can influence both the structure of the adsorbent and the adsorbate, as well as the adsorption mechanism.

Fig 10 shows the percentage removal of Bezanyl Yellow dye on DD1 and Z1 adsorbents at different pH values at 20 °C. The adsorption capacity was favored by the pH increase from 2 to 7, with a maximum value of 55.6 mg/g and 95 mg/g for DD1 and Z1 respectively, followed by a small decrease for both adsorbents at pH 11.

In acidic media, the hydronium ions H_3O^+ are in competition with active sites on the surface of the adsorbent, which results in protonation of the adsorbent's active sites and leads to a slight increase in the adsorption capacity of the anionic dye. By increasing the solution pH, the density of positive charges on the surface sites of the adsorbent slightly decreased, which resulted in the decrease of the adsorption of Bezanyl Yellow on zeolite Z1. The maximum adsorption of Bezanyl Yellow at pH 7 can be attributed to the electrostatic interactions between the positively charged surface of the adsorbent and the negatively charged anions of dye. A similar trend was found by Naushad et al. (2019) and Sanxin et al. (2019). However, the removal rate in the case of DD1 did not exceed 55%. A similar tendency was reported by Zen et al. (2018) for kaolin DD3. This would indicate that pH doesn't have a strong influence on the adsorption and that adsorption capacity would be more related to the pore structure.

Fig10: Effect of pH on the adsorption of Bezanyl Yellow, (C_o= 25 mg / L, pH= 6, T= 20 ° C, contact time= 120 min)

3.3 Proposed adsorption mechanism

All these results show that the adsorption capacity of Z1 zeolite is higher than for DD1 kaolin. The dye molecules binding on the surface of the zeolite can be represented as an interaction of the oxygen atoms of the zeolite with the sulfonate groups of Bezanyl Yellow molecules. Knowing that the dyes exhibit a lower topological polar surface a value (177 $Å^2$) (PubChem, 2015) and low-sized groups of atoms **(**See the 3D structure depicted in

Table1**)**, the high polar groups in Bezanyl Yellow (sulfonate group) would interact easily with a highly-polar adsorbent surface**.** Therefore, the small particles of Z1 zeolite retained much more Bezanyl Yellow molecules when compared to DD1 kaolin (the particle size range for DD1 is 8-20 μm), and the rate of adsorption was very fast.

Based on these assumptions, a schematic representation is proposed (**Fig 11)**. The adsorption mechanism of the Bezanyl Yellow into the interlayer space of Z1 Zeolite type 13X can be attributed to various types of interactions, and as shown in **Fig 11**, the compound could be partly or fully coated and embedded within the zeolite.

Fig11: Schematic representation in different views of the possible interactions between Bezanyl Yellow and Z1 zeolite type 13X.

3.4 Comparative study

Table 4 lists the rate of Bezanyl Yellow dye removal by various microporous adsorbents reported in the literature. As can be seen in Table 4 and what is mainly reported in studies on the adsorption of anionic molecules onto zeolite, the zeolites that are modified show higher adsorption capacities than unmodified zeolites. This is due to the repulsion between the negatively charged zeolite and the anionic dye molecules which is a hindrance to the adsorption (Alver and Metin, 2012). Contrary, one can observe that the zeolite 13X synthesized from DD1 kaolin exhibits a high adsorption capacity for Bezanyl Yellow, which indicates that anionic dye adsorption using unmodified zeolites is possible and can even be efficient. This was also reported for example by Rodrigues Bertolini et al. (2015) for unmodified zeolite synthesized from coal fly ash that removed 76% Acid Orange 8 dye which is in the same range as the modified zeolites removing 84% of dye. This is probably due to interactions between Si-O and O-H active sites on zeolite and the -SO3- and -N=N- groups of the dye as explained by Rodrigues Bertolini et al. (2015). In addition, particle size is an important parameter that influences the adsorption capacity. Small sized particles exhibit larger reactive surfaces, which enhances the adsorption capacity. On one hand, as can be observed on SEM micrographs, the zeolite synthesized from DD1 forms a material with smaller sized particles (around 1μm) compared to DD1 (8-20 μm), which induces a larger reactive surface and a higher adsorption potential. On the other hand, the structure observed in the SEM images shows that the zeolite aggregates form a very large number of accessible pores compared to DD1. That may explain the good results obtained with the unmodified zeolite synthesized from DD1 kaolin.

Thus, from these data, it can be said that zeolite Z1 synthesized from DD1 kaolin is an effective and promising material for adsorption of anionic dyes.

Table 4: Adsorption capacities of Acid Yellow on various adsorbents

Adsorbent	Dye	Q	Removal	Reference
Our work Zeolite Z	Bezanyl Yellow	50 mg/g	90%	/
Zeolite A	Bezanyl Yellow	2.8mg/g	26%	Fardjaoui et al, (2017)
CTMAB-Bentonite	Acid golden Yellow	/	93%	Yan et al., (2015
Activated Carbon	Acid Yellow RR	/	70%	Rita et al, (2012)
Activated rice husk	Acid Yellow 36	/	80–45%	Imam et al, (2003)

4. Physicochemical characterization of textile effluents before and after adsorption

The main physicochemical characteristics of the raw effluent supplied by the "EATIT" textile company in Batna is given in **Table 5**. The effluent before treatment has a dark green color with a very unpleasant smell that is due to the existence of either chemicals or decomposing organic matter.

Table 5: Characteristics of EATIT textile effluent

Physicochemical characteristics	Textile effluent
Color	Dark
Odor	Bad smell
pH	7.70
Conductivity (mS/cm)	1.5
COD (mg O_2/L)	869
BOD_5 (mgO_2/L)	203
TSS	20
SO_4^{2-} (mg/L)	650
NH_4^+ (mg/L)	0.18
NO_2^- (mg/L)	0.33
PO_4^{3-} (mg/L)	1.33

The effluent is very loaded with organic matter, sulfates, phosphates and nitrite. The physicochemical characteristics of this effluent vary depending on the nature of the fabric washed and the chemicals added for washing (enzymes, softeners, bleach ...), and mainly the color of the fabric. We can note that all measured parameter values are higher than the Algerian standards for release in the sewage network (**Table 6)**.

We applied the adsorption of the effluent on DD kaolins (DD1, DD2, and DD3) and Z zeolites for an adsorbent mass value of 0.1 g. The results of the physicochemical characteristics of the effluent after treatment are summarized in **Table 6.**

Table 6: Physicochemical characteristics of the effluent after treatment (m= 0.1g)

Parameter		Raw effluent	Effluent after adsorption on :					
			DD1	DD2	DD3	Z1	Z2	Z3
Color	/	Dark green	Almost colored	Little colored	Little colored	Very little colored	Little colored	Little colored
Odor	/	Unpleasant	No odor	No odor	No odor	No odor	No odor	No odor
pH	/	7.70	7.92	8.03	8.06	7.90	7.95	8.16
Conductivity	S/cm	1.5	1.4	1.5	1.4		1.5	1.1
TSS	mg/l	20	3	9	4	0.1	1	0.5
COD	mg/l O_2	869	481	525	555	565	569	587
BOD_5	mg/lO_2	203	63	/	/	80	/	/
$SO4^{2-}$	mg/l	650	483	500	549	423	469	566
NH_4^+	mg/l	0.18	0.12	0.13	0.15	0.10	0.11	0.14
NO_2^-	mg/l	0.33	0.16	0.23	0.28	0.15	0.20	0.21
PO_4^{3-}	mg/l	1.13	0.83	0.97	1.08	0.75	0.88	1.07

TSS: Total suspended solids

COD: Chemical oxygen demand

BOD_5: Biochemical oxygen demand in five days

Table 6 shows that, whatever the adsorbent used, the COD values were reduced by approximately half compared to the value of the effluent before treatment (869 mg/L). They are however not low enough to meet the standard values. Similarly, the BOD_5 decreased after treatment for all the adsorbents and especially in the case of DD1 and Z1 zeolite. The final COD values highly decreased to 481 mg/ L and 565 mg/ L for DD1 kaolin and Z1 zeolite respectively, while BOD_5 values decreased slightly from 203 mg/L to 63 mg/L and 80 mg / L of O_2 for DD1 kaolin and Z1 zeolite respectively. Therefore, it can be said that adsorption on kaolin DD1 and zeolite Z1 is an effective process for pollutants removal from textile wastewater. This potential of COD removal from wastewater

by zeolite was also reported by Genethliou et al. (2021). This can be explained in our case by the high surface area in the large pores formed by DD1 and Z1 aggregates as could be observed on the SEM micrographs, in addition to the surface area provided by external platelets and crystals of DD1 and Z1, and internal pores and channels of Z1 zeolite. This is in line with the observations of Genethliou et al. (2021) who noticed a higher COD removal efficiency by using bigger particle sizes.

The effluent to be treated is alkaline due to the negative charges of colloids and anionic dyes (pH =12). After treatment pH became close to the neutralization whatever the adsorbent used.

The concentrations of nitrites, sulfates, ammonium, and phosphates decreased after treatment and this was more significant in the case of kaolin DD1 and the Z1 zeolite, reaching values within the Algerian standards set for effluent treatment.

On the other hand, we measured some physicochemical parameters after adsorption, using 1 g of DD1 and Z1 zeolite (**Table 7)**.We observed that increasing the mass of the adsorbent, there is a significant decrease of the physicochemical parameter values. Thus, a higher dose of adsorbent reduces the degree of pollution of the effluent, which enables some parameters values to meet the standards for reuse in agriculture.

Table 7: Physicochemical characteristics of the effluent after treatment (m= 1g)

Parameters	Unit	Effluent after adsorption on :	
		DD1	Z1
Color	/	Colourless	Colourless
Odor	/	No odor	No odor
SO_4^{2-}	mg/l	320	210
NH_4^+	mg/l	0.9	0.6
NO_2^-	mg/l	0.11	0.8
PO_4^{3-}	mg/l	0.25	0.20

5. Theoretical and Computational Study

Recently, molecular docking softwares proved to be relatively simple, rapid, and economical techniques for studying the inclusion phenomena. For preparing the starting system, the initial structure for the 13X Zeolite was extracted from the Database of Zeolite Structures (IZA-SC, 2017). At first, all calculations, including geometry optimizations, frequency calculations and rigid scan for isolated monomers (zeolite and Bezanyl yellow), and 1:1 complex, were performed using the PM6 semi-empirical method (Stewart 2007) as implemented in *Gaussian 09 (*E.01) software package (Frisch et al. 2009).

Fig 12: The proposed mechanism of inclusion process of Bezanyl yellow into Zeolite

The isolated compounds (zeolite and Bezanyl yellow) were optimized in the gas phase. The conformational analysis of various insertions of the Bezanyl yellow compound inside the host's cavity of zeolites is assumed **(Fig 12)** by scanning along the Z-axis at a distance that equals 9 Å from the center. The side views of the optimized structures can be seen in **Fig 13 (a, b, c)**. The guest molecule of Bezanyl yellow was systematically moved from the outside to the inside of the host cavity along the -Z axis with a displacement equal to 9 Å, and with an increment of 0.1 Å.

Fig 14 gives the energy variation (ΔE) as a function of the displacements of the guest molecule inside the cavity. According to the relative values of the total energies, the geometries of the complexes obtained after each displacement show a reasonable pattern indicating the increased stability of the complex, which is attributed to the formation of weak non-covalent bonds.

It should be mentioned that the semi-empirical method (PM6) was used due to the size of the studied system.

Fig13: Geometric structures of the side views of the optimized structures of ***Bezanylyellow@zeolite*** complexes.

Fig 14: Evolution of the total energy during the inclusion process, in the a-orientation.

6. Conclusion

This study was carried out to investigate the potential of Djebel Debagh (DD) natural and modified kaolins to treat raw textile effluents.

The kinetics of Bezanyl Yellow anionic dye adsorption on DD kaolins and Z zeolites indicates that they are good adsorbents in an aqueous solution. The adsorption is influenced by parameters such as the pH of the solution, the temperature, the initial concentration of the dye, and the mass of the adsorbent. Among adsorbents, the best results were recorded for kaolin DD1 and zeolite Z1. The characterization of DD kaolins and Z zeolites by different analysis methods allowed to better understand the retention mechanism of the anionic dye. The adsorption of Bezanyl Yellow by kaolin DD1 and zeolite Z1 increased with the increase of the initial concentration of the dye and of the mass of the adsorbent, and moreover was improved at pH= 7. The Z1 zeolite synthesized by kaolin DD1 as an adsorbent exhibits a higher potential for a real application in wastewater treatment. All these observations

indicate that DD natural kaolins and 13X type zeolites (Z) synthesized from DD kaolins are promising materials for applications in anionic dye adsorption and in the treatment of textile industries' effluents. This is an important result because the adsorption of the dye takes place efficiently although the surface of the adsorbents and the dye have overall negative charges. Surface modification of the kaolin and zeolite is not necessary, which is an advantage from the point of view of durability for the treatment by adsorption on these materials. The second important information derived from the experiments and observations is that the porous structure of the zeolites, the particle size, as well as the structuring of the particle aggregates, and thus the specific surface area offered for adsorption, play a major role in the adsorption, in conjunction with the polar nature of the dye and the adsorbent surfaces.

The third important aspect of this work is the use of Density Functional Theory calculations on the negatively charged zeolite and dye, which has not yet been treated in the literature. The simulations allowed us to propose mechanisms for the dye inclusion process in the zeolite cavities. Moreover, energy variation calculations during the inclusion indicate that the complex becomes stable through weak non-covalent bonds. Thus the experimental study carried out in this work is in good agreement with the theoretical results indicating that the efficient process of anionic dye adsorption on Z zeolite is a free and energetically favorable process.

Acknowledgements

This paper is supported by the PRIMA program under grant agreement No2024 - TRUST project. The PRIMA program is supported by the European Union. It was also supported by the General Directorate of Scientific Research and Technological Development (DGRSDT) in Algeria under the authority of the Minister in charge of scientific research and France (National Research Agency, ANR).

The authors would like to gratefully acknowledge Mrs. Rabia GUERAICHE (Engineer in the EATITcompany) for providing the textile effluent, and the industrial analysis and materials engineering laboratory (LAIGM) in Guelma for performing the COD analyses.

References

AFNOR NF EN 1899-2 standard 1998. Determination of biochemical oxygen demand after n days (BOD), part 2: Method for undiluted samples (Classification index T90-103-2).

Alver E, Metin A Ü (2012) Anionic dye removal from aqueous solutions using modified zeolite: Adsorption kinetics and isotherm studies. Chem. Eng. J.https://doi.org/10.1016/j.cej.2012.06.038

APHA 1998. American Public Health Association; Standard methods for the exmination of water and waste water; 20th edition, Washington

Aiello R, Colella C, Casey DG, Sand LB (1984) Proceedings of the 5th International Conference on Zeolites, Heyden, London, 1984, p. 49

Akolekar D, Chaffee A, Howe R. F (1997). The transformation of kaolin to low-silica X zeolite. Zeolites. https://doi.org/10.1016/S0144-2449(97)00132-2

Alshahidy BA, Abbas AS (2021) Comparative Study on the Catalytic Performance of a 13X Zeolite and its Dealuminated Derivative for Biodiesel Production. Bull Chem React Engcatal. https://doi.org/10.9767/bcrec.16.4.11436.763-772

Barrer RM, Beaumont R, Colella C (1974). Action of some basic solutions of metakaolinite and kaolinite. J Chem Soc Dalton Trans. 934-941(1974).

Baur W H (1964) On the cation and water positions in faujasite .Am Min 49 (1964) 697-704.

Ben Arfi R, Karoui S, Mougin K et al (2017) Adsorptive removal of cationic and anionic dyes from aqueous solution by utilizing almond shell as bioadsorbent. Euro-Mediterr J Environ Integr. https://doi.org/10.1007/s41207-017-0032-y

Calligaris M, Nardin G, RandaccioL.(1982) Cation-site location in a natural chabazite Acta Crystallogr B38 (1982) 602-605

Candamano S, Policicchio A, Macario A et al (2019) CO_2 adsorption investigation on an innovative nanocomposite material with hierarchical porosity. J NanosciNanotechnolhttps://doi.org/10.1166/jnn.2019.16650

Casaburi O, Petrosino F, Marra F (2021) Modeling Aspects in Simulation of Mef Processing of Solid Behaving Foods, Chem Eng Trans. https://doi.org/10.3303/CET2187038

Chen D, Hu X, Shi L et al (2012) Synthesis and characterization of zeolite X from lithium slag, Appl. Clay Sci. http://dx.doi.org/10.1016%2Fj.clay.2012.02.017

Chowdam R (2016) Rapid and complete degradation of sulphur mustard adsorbed on M/zeolite-13X supported (M = 5 wt% Mn, Fe, Co) metal oxide catalysts with ozone. RSC Adv. https://doi.org/10.1039/C6RA17215F

Curcio S, Petrosino F, Morrone M, De Luca, G (2018) Interactions between Proteins and the Membrane Surface in Multi scale Modeling of Organic Fouling. J Chem Inf Modeli, https://doi.org/10.1021/acs.jcim.8b00298

Fardjaoui NH, El Berrichi FZ, Ayari F (2017) Kaolin-issued zeolite A as efficient adsorbent for Bezanyl Yellow and Nylomine Green anionic dyes, MicroporMesopor Mat http://dx.doi.org/10.1016%2Fj.micromeso.2017.01.008

Frisch JM et al (2009). Gaussian 09 (Gaussian, In, Wallingford CT,2009).

Genethliou C, Triantaphyllidou IE, Giannakis D et al (2021) Simultaneous removal of ammonium nitrogen, dissolved chemical oxygen demand and color from sanitary landfill leachate using natural zeolite. J Hazard Mater. https://doi.org/10.1016/j.jhazmat.2020.124679

Hartati H, et al (2020) A review on synthesis of kaolin-based zeolite and the effect of impurities. J Chin Chem Soc. http://dx.doi.org/10.1002/jccs.201900047

Hassan I, Antao S M, Parise J B (2004) Sodalite: High-temperature structures obtained from synchrotron radiation and Rietveld refinements. Am Min 89 (2004) 359-36

Imam HM, Hameed BH, Ahmad AL (2003) Aqueous-Phase Adsorption of Phenolic Compounds on activated carbon. In: Proceedings. The 17th Symposium of Malaysian Chemical Engineers, 29-30 December 2003

IZA-SC (2017) https://europe.iza-structure.org/

Ma Y, Yan C, Alshameri A et al (2014) Synthesis and characterization of 13X zeolite from low-grade natural kaolin. Adv Powder Technol. https://doi.org/10.1016/j.apt.2013.08.002.

Naushad M, Alqadami A et al (2019) Adsorption of textile dye using para-aminobenzoic acid modified activated carbon: Kinetic and equilibrium studies; JMolLiq. https://doi.org/10.1016/j.molliq.2019.112075

NF EN 872 (2005). Water quality - Determination of suspended solids.

Othmani A, Kesraoui A, Seffen M (2017) The alternating and direct currenteffect on the elimination of cationic and anionic dye from aqueous solutions by electrocoagulation and coagulation flocculation. Euro-Mediterr J Environ Integr. https://doi.org/10.1007/s41207-017-0016-y

Petrosino F, Hallez Y, De Luca G, Curcio S (2020) Osmotic pressure and transport coefficient in ultrafiltration: A Monte Carlo study using quantum surface charges. Chem Eng Sci, https://hal.archives-ouvertes.fr/hal-02863893

Petrosino, F, Curcio S, Chakraborty S, De Luca, G (2019) Enzyme Immobilization on Polymer Membranes: A Quantum and Molecular Mechanics Study. Computation, https://doi.org/10.3390/computation7040056

.

Petschick R, Kuhn G, Gingele F (1996) Clay mineral distribution in surface sediments of the South Atlantic: sources, transport, and relation to oceanography, J Mar Geol. https://doi.org/10.1016/0025-3227(95)00148-4

Pub©Chem (2015), Open Chemistry Database, CID 23668793.

Qiang Z, Yan Z, Jing O, Yi Z, Yang H, Chen D (2018) Chemically modified kaolinite nanolayers for the removal of organic pollutants. Appl Clay Sci. https://doi.org/10.1016/j.clay.2018.03.009

Ramdani , Taleb Z, Guendouzi A, Kadeche A, Herbache H, Mostefai A, Taleb S, Deratani A (2020). Mechanism study of metal ion adsorption on porous hydroxyapatite: experiments and modeling. Can J Chem, https://doi.org/10.1139/cjc-2019-0315

Rita K (2012) Adsorption of yellow dye: Acid yellow RR from its aqueous solution using two different samples of activated carbon by static batch method. J Nat Sci. http://dx.doi.org/10.4236/ns.2012.42016

Rodrigues Bertolini T C, Reis Alcântara R, de CarvalhoIzidoro J, Alves Fungaro D (2015)Adsorption of Acid Orange 8 Dye from Aqueous Solution Onto Unmodified and Modified Zeolites. Orbital: Electron. J. Chem. http://dx.doi.org/10.17807/orbital.v7i4.76

Sandeep A, Lakhera SK, et al (2015) Synthesis and Characterization of 13X Zeolite/ Activated Carbon Composite. J Chem Tech Research. Vol.7, No.3, pp 1364-1368.

Sanxin N, Xiaokang X, Zheng W et al (2019) Enhanced removal performance for Congo red by coal-series kaolin with acid treatment. Env Tech. https://doi.org/10.1080/09593330.2019.1670269

Schwanke AJ, Balzer R, Pergher S (2019) Microporous and Mesoporous Materials from Natural and Inexpensive Sources. In: Martínez L., Kharissova O., Kharisov B. (eds) Handbook of Ecomaterials. Springer, Cham. https://doi.org/10.1007/978-3-319-68255-6_43

Shigemoto N, Hayashi H, Miyaura K (1993) Selective formation of Na-X zeolite from coal fly ash by fusion with sodium hydroxide prior to hydrothermal reaction, J. Mater. https://doi.org/10.1007/BF00414272

Singer A, Berkgaut V (1995) Cation Exchange Properties of Hydrothermally Treated Coal Fly Ash. Environ. Sci. Technol. https://doi.org/10.1021/es00007a009

Slatni I, El BerrichiFZ, Duplay J et al (2020) Mesoporous silica synthesized from natural local kaolin as an effective adsorbent for removing of Acid Red 337 and its application in the treatment of real industrial textile. Environ Sci Pollut Res. https://doi.org/10.1007/s11356-020-08615-5

Stewart JJP (2007) Optimization of parameters for semi empirical methods V: Modification of NDDO approximations and application to 70 elements. J Mol Model.https://doi.org/10.1007/s00894-007-0233-4

Suquet H (1989) Effects of dry grinding and leaching on the crystal structure of chrysotile. clays clay Miner. https://doi.org/10.1346/CCMN.1989.0370507

Treacy MMJ, Higgins JB (2007) Collection of simulated XRD powder patterns for Zeolites. Fifth (5th) Revised Edition. Elsevier https://doi.org/10.1016/B978-0-444-53067-7.X5470-7

Villaquirán-Caicedo MA, De Gutiérrez RM, Gordillo M, Gallego NC (2016). Synthesis of zeolites from a low-quality Colombian kaolin. Clays Clay Miner. https://doi.org/10.1346/CCMN.2016.0640201

Alkan, M. (2007). *Adsorption kinetics and mechanism of cationic methyl violet and methylene blue dyes onto sepiolite*. *75*. https://doi.org/10.1016/j.dyepig.2006.07.023

Yan, L., Qin, L., Yu, H., Li, S., Shan, R., & Du, B. (2015). Adsorption of acid dyes from aqueous solution by CTMAB modified bentonite: Kinetic and isotherm modeling. *Journal of Molecular Liquids*, *211*, 1074–1081. https://doi.org/10.1016/j.molliq.2015.08.032

Zene S, El Berrichi FZ, Abidi N et al (2018) Activated kaolin's potential adsorbents for the removal of Derma Blue R67 acid dye: kinetic and thermodynamic studies. Desalination Water Treat. https://dx.doi.org/10.5004/dwt.2018.21996

Zhan BZ, White MA, Lumsden M et al (2002) Control of Particle Size and Surface Properties of Crystals of NaX Zeolite. Chem Mater. https://doi.org/10.1021/cm011635f

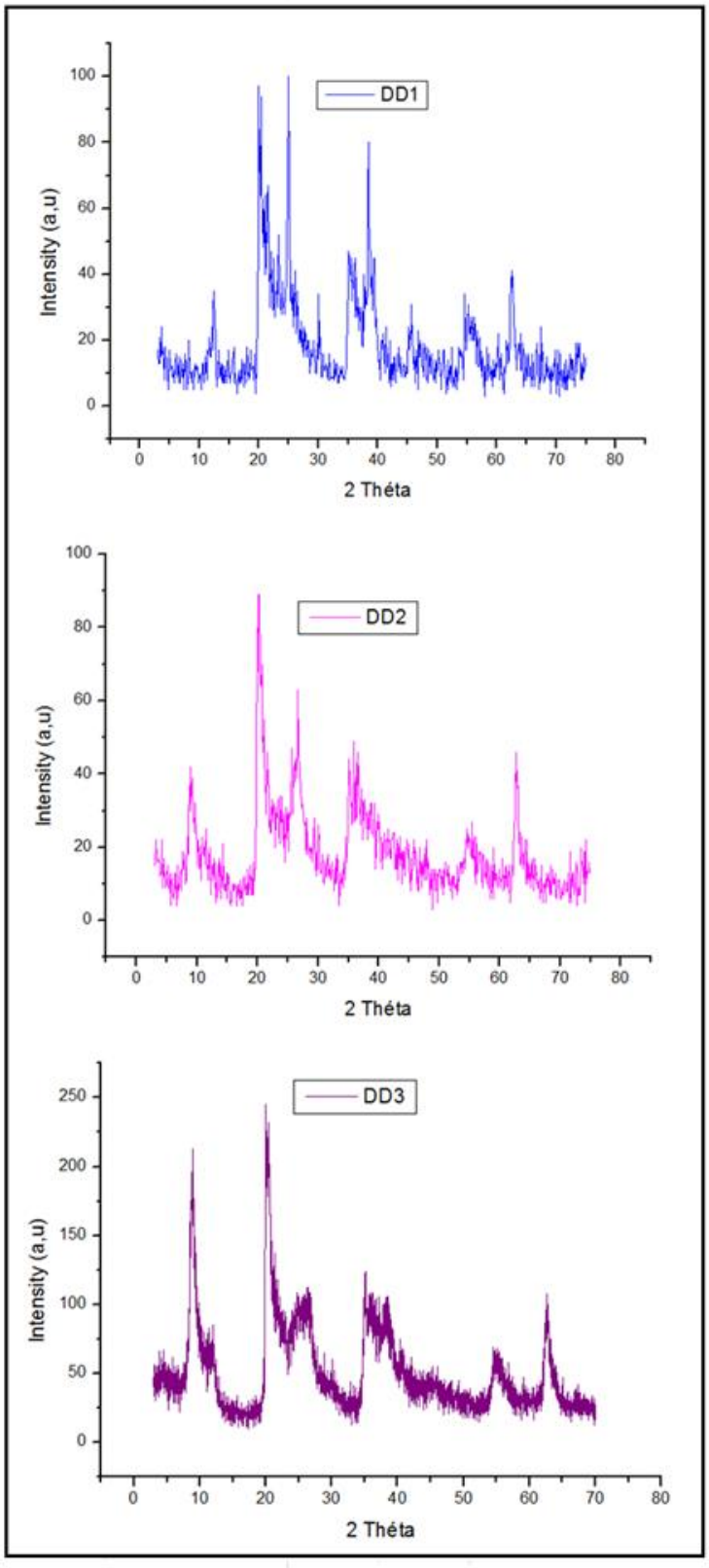

Fig1. JPG: XRD patterns of DD kaolins

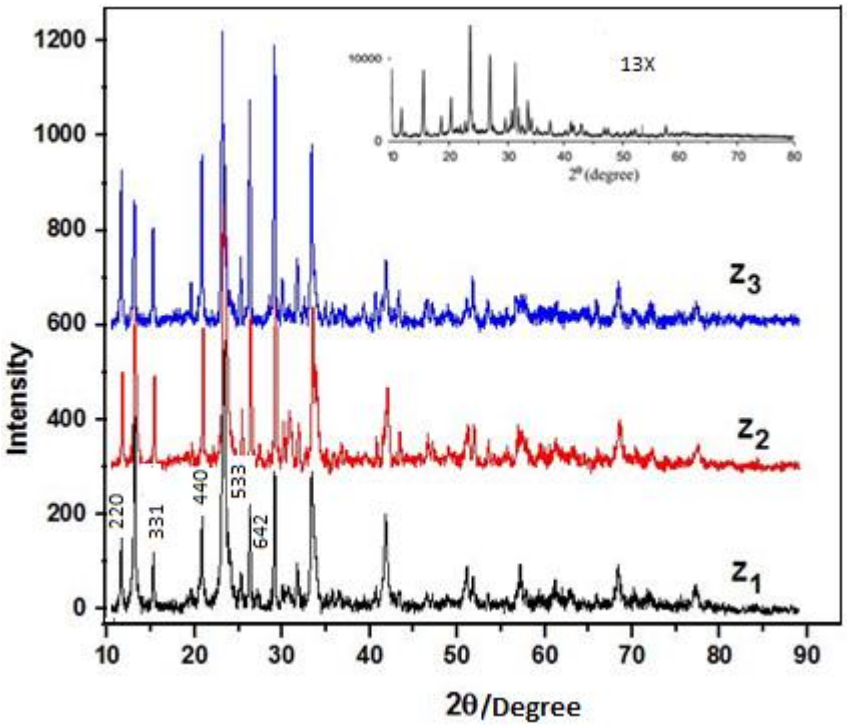

Fig2 .OPJ: XRD pattern of Z1, Z2, Z3 zeolites and standard 13X zeolite

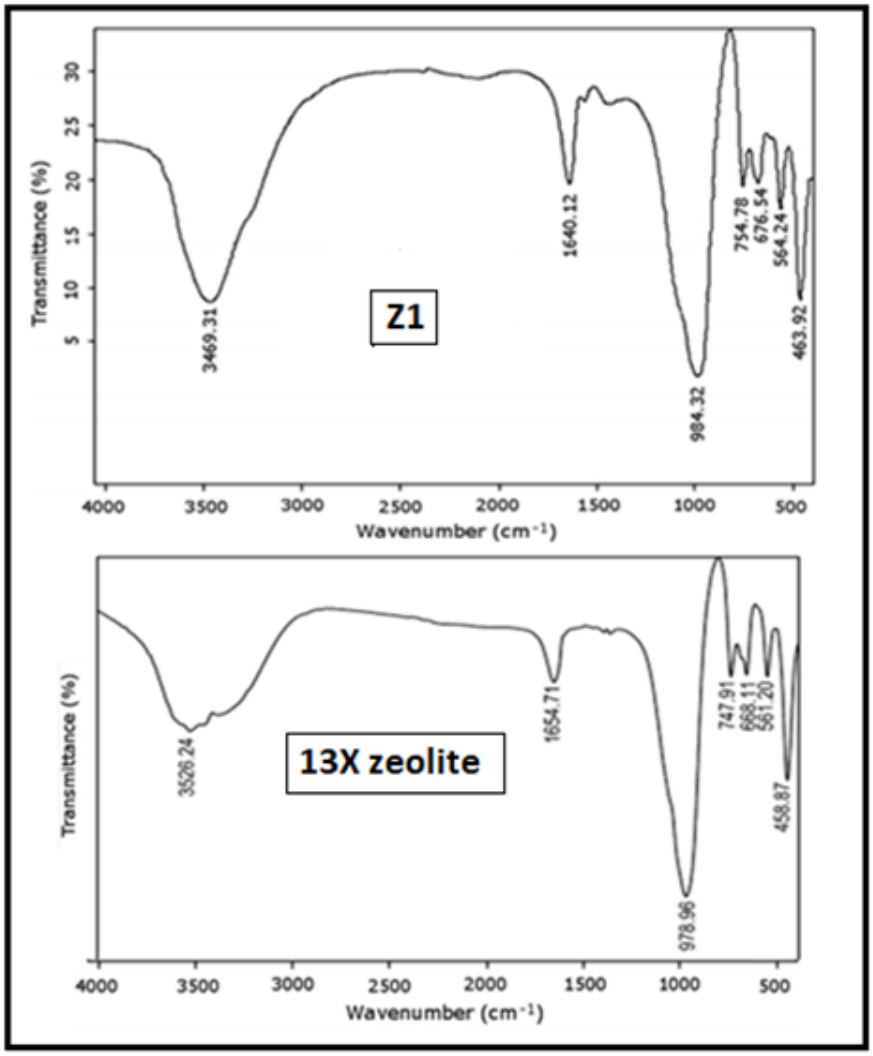

Fig3 .JPG: FTIR spectra of Z1 zeolite and 13 X Zeolite from the literature (Chen et al. 2012)

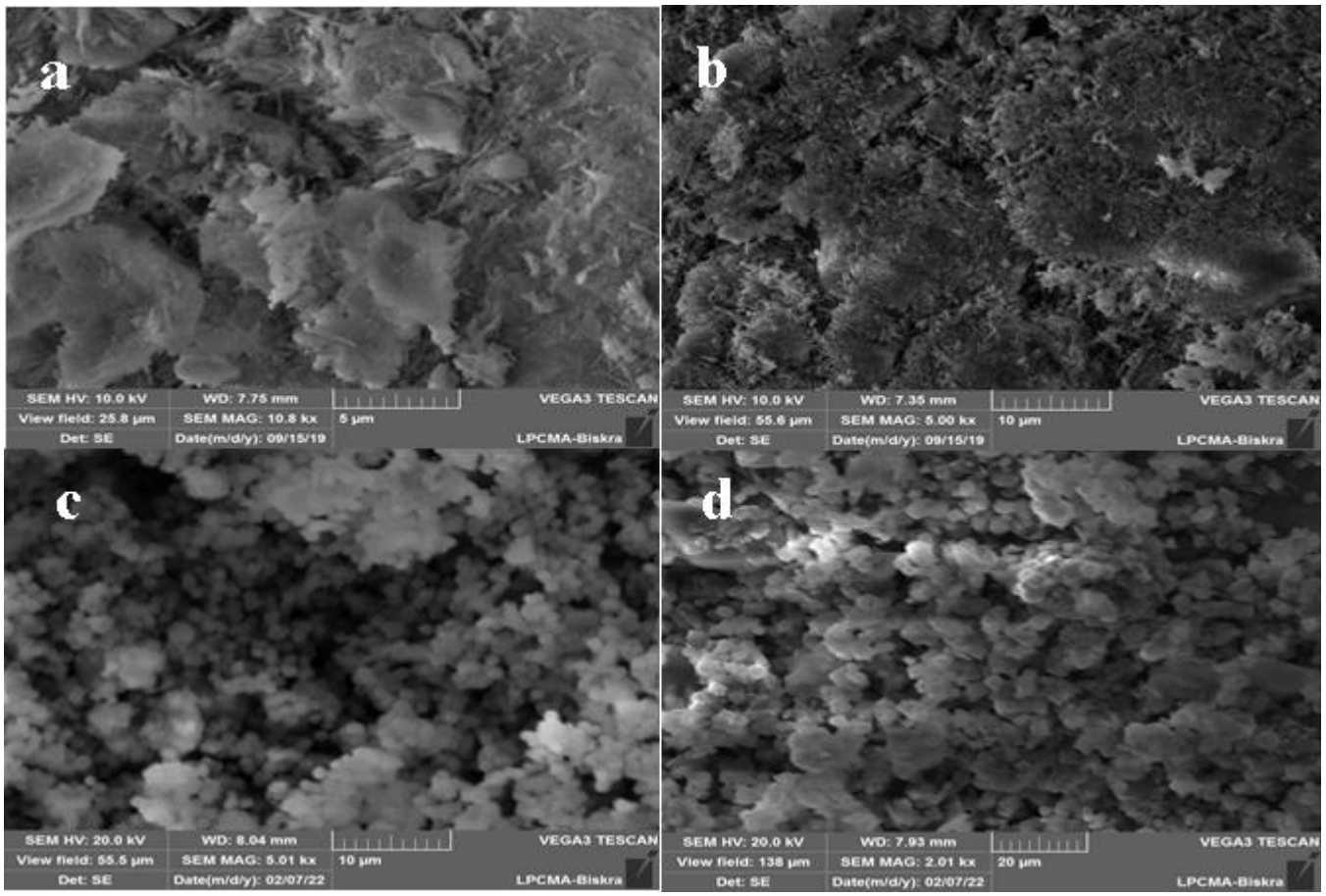

Fig4. JPG: Scanning electron micrographs of DD1 kaolin (a, b) and Z1 zeolite (c, d) at different magnifications

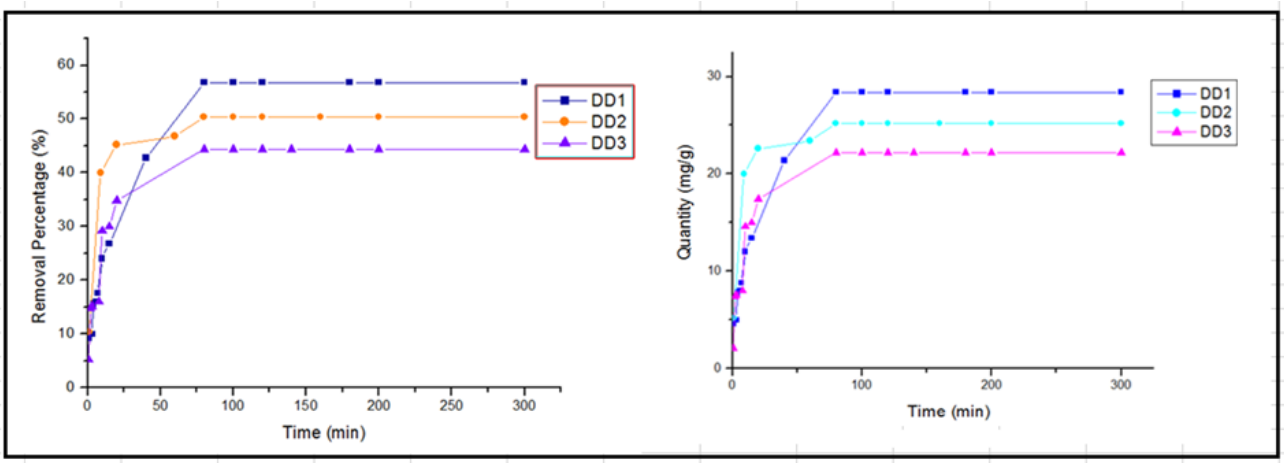

Fig5.JPG: Effect of the contact time in the removal of Bezanyl Yellow on DD kaolins (m = 0.1g, pH = 6, C_o = 25 mg / L, T = 20 °C)

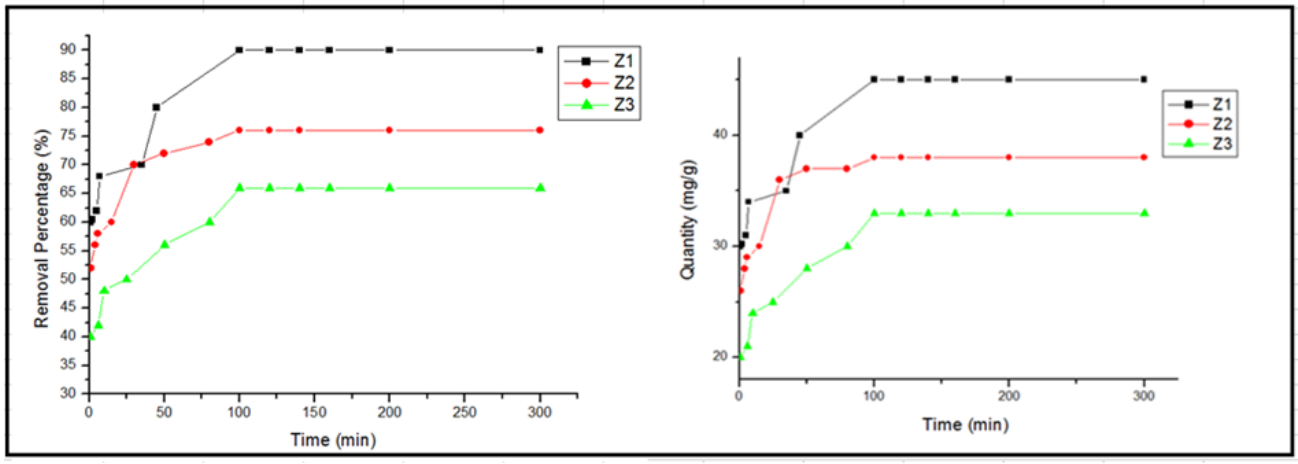

Fig6. JPG: Effect of the contact time in the removal of Bezanyl Yellow on Z zeolites (m = 0.1g, pH = 6, Co = 25 mg / L, T = 20 °C).

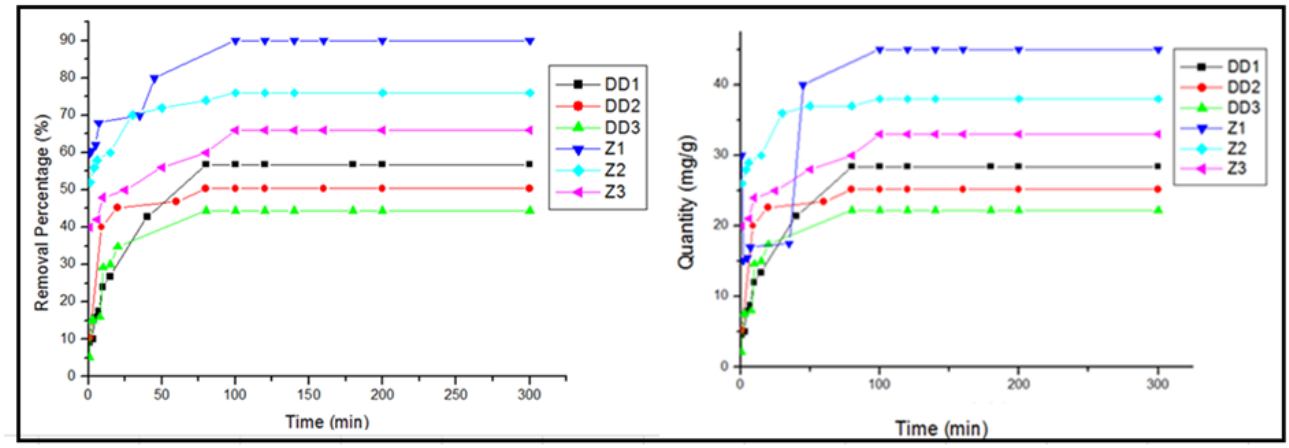

Fig7.JPG: Effect of adsorbent nature on the removal of Bezanyl Yellow dye (m = 0.1g, pH = 6, C_o = 25 mg / L, T = 20 ° C)

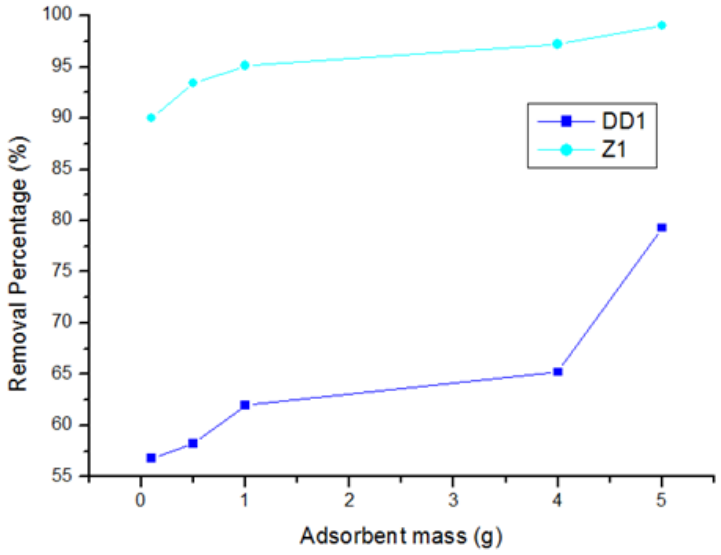

Fig8 .JPG: Effect of the mass of kaolin DD1 and the zeolite Z1 on the adsorption of Bezanyl Yellow, (C_o = 25 mg / L, pH = 6, T = 20 °C, contact time = 120 min)

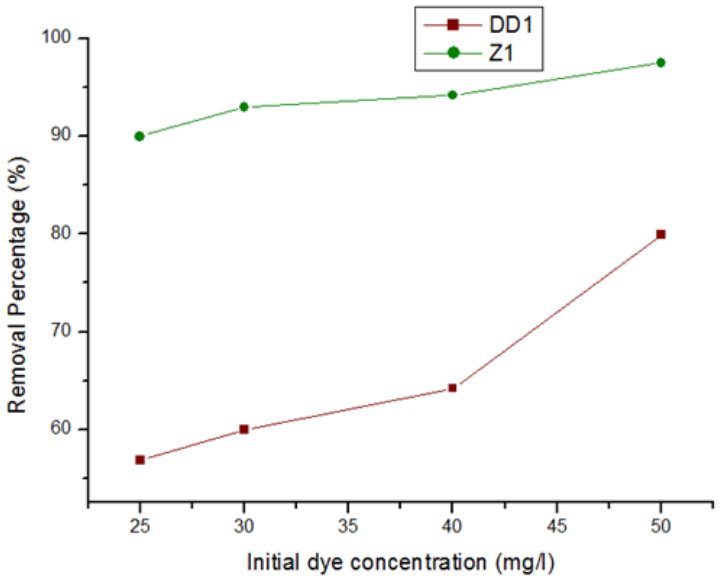

Fig9 .JPG: Effect of initial dye concentration of Bezanyl Yellow, (m= 0.1g, pH= 6, T = 20 °C, contact time = 120 min)

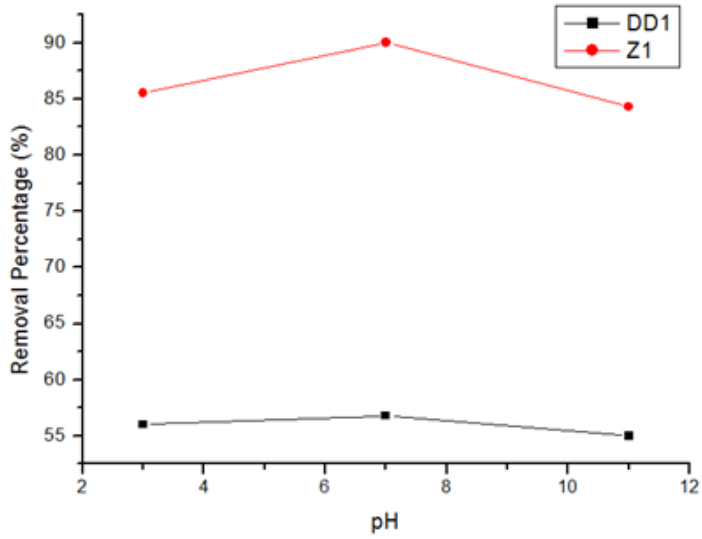

Fig10 .JPG: Effect of pH on the adsorption of Bezanyl Yellow, (Co = 25 mg / L, pH = 6, T = 20 °C, contact time = 120 min)

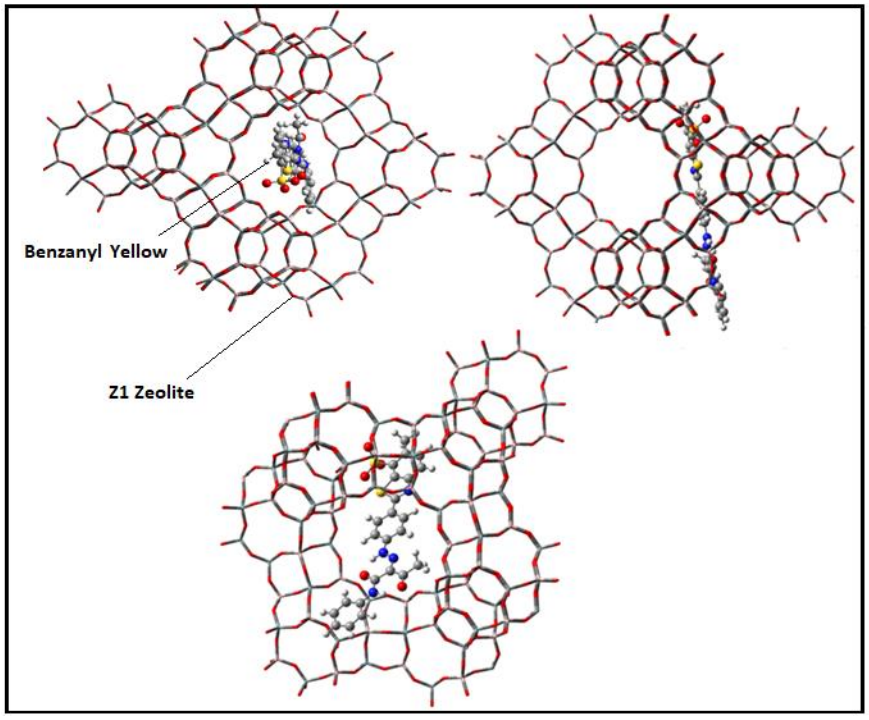

Fig11. JPG: Schematic representation in different possible interactions between Bezanyl Yellow and Z1 zeolite (13X type).

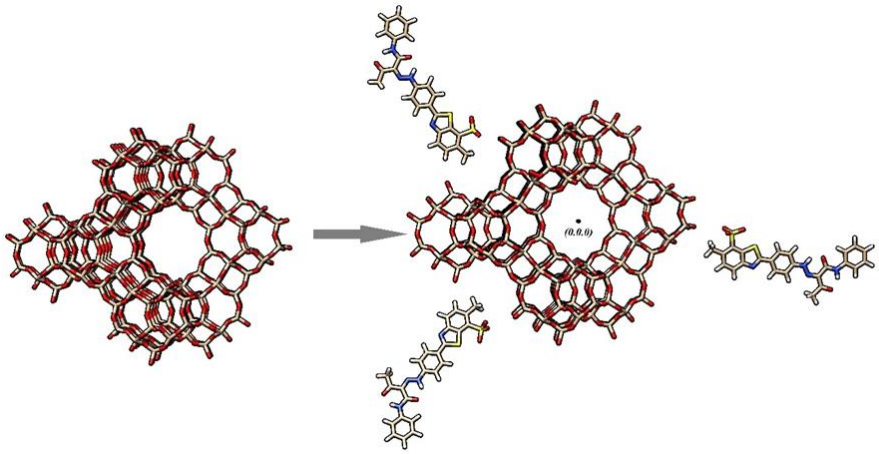

Fig12 .JPG: The proposed mechanism of inclusion process of Bezanyl yellow into Zeolite

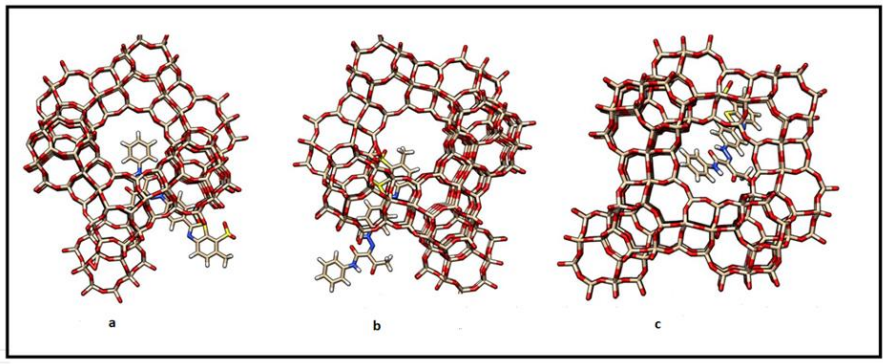

Fig13 .JPG: Geometric structures of the side views of the optimized structures of Bezanyl yellow @ zeolite complexes (a, b, c)

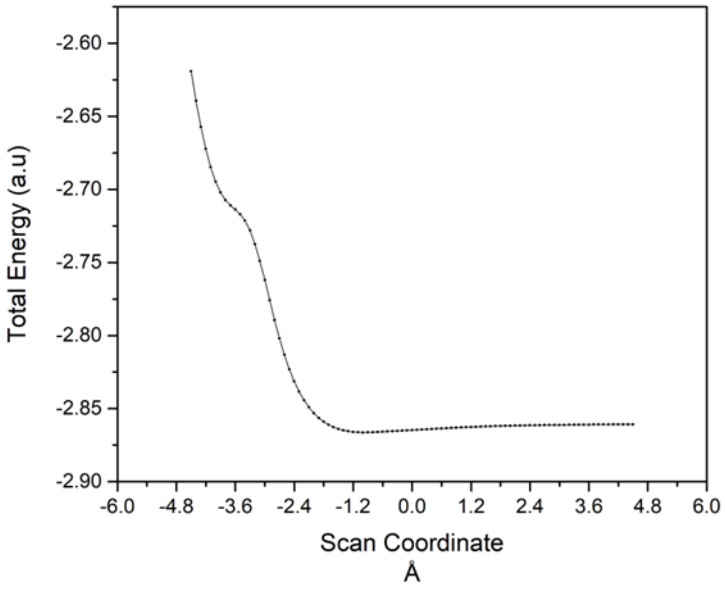

Fig14. JPG: Evolution of the total energy during the inclusion process, in the a-orientation.